




REVIEW ARTICLE

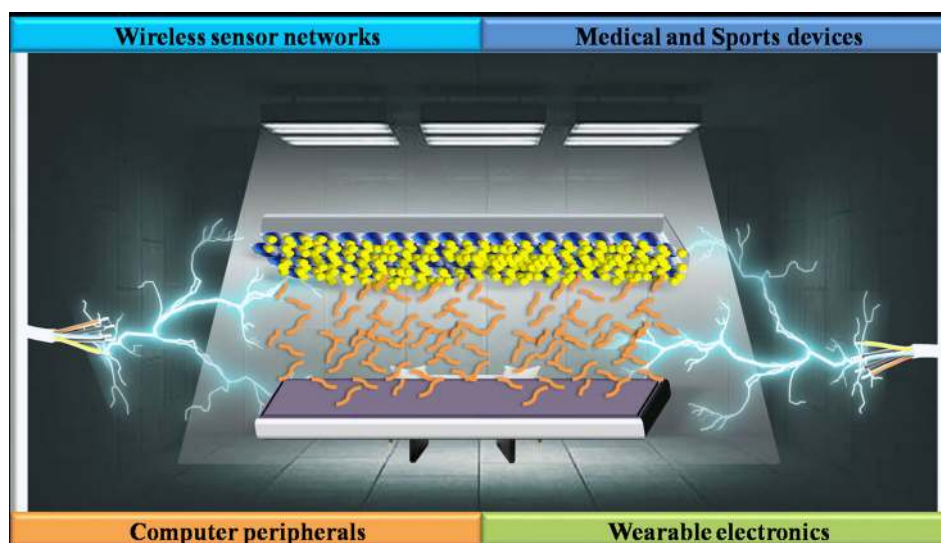
Dye-Sensitized Solar Cell for Indoor Applications: A Mini-Review

DHEERAJ DEVADIGA,¹ M. SELVAKUMAR ^{1,3} PRAKASHA SHETTY,¹
and M.S. SANTOSH²

1.—Department of Chemistry, Manipal Institute of Technology, Manipal Academy of higher education, Manipal, Karnataka 576104, India. 2.—Centre for Incubation, Innovation, Research, and Consultancy (CIIRC), Jyothy Institute of Technology, Tataguni, Off Kanakapura Road, Bangalore, Karnataka 560082, India. 3.—e-mail: chemselva@rediffmail.com

Lightweight computing technologies such as the Internet of Things and flexible wearable systems have penetrated our everyday lives exponentially in recent years. Without a question, the running of such electronic devices is a major energy problem. Generally, these devices need power within the range of microwatts and operate mostly indoors. Thus, it is appropriate to have a self-sustainable power source, such as the photovoltaic (PV) cell, which can harvest indoor light. Among other PV cells, the dye-sensitized solar cell (DSSC) has immense capacity to satisfy the energy demands of most indoor electronics, making it a very attractive power candidates because of its many benefits such as readily available materials, relatively cheap manufacturing methods, roll-to-roll compatibility, easy processing capabilities on flexible substrates and exceptional diffuse/low-light performance. This review discusses the recent developments in DSSC materials for its indoor applications. Ultimately, the perspective on this topic is presented after summing up the current progress of the research.

Graphic abstract



Key words: Dye-sensitized solar cell, indoor application, sensitizers, photoanode, electrolyte, Counter electrode

Abbreviations

DSSC	Dye-sensitized solar cell
PV	Photovoltaic
CE	Counter electrode
PCE	Power conversion efficiency

INTRODUCTION

Humans have introduced more carbon dioxide into the environment than the earth's trees have been able to recycle since the industrial revolution, resulting in an increase in the global temperature. Photovoltaics (PVs) play a major role in energy harvesting and in realizing a low-carbon society.¹⁻⁶ Alternative PVs are emerging alongside widely commercialized semiconductor technologies based on crystalline and thin-film silicon solar cells.⁷⁻¹⁴ In addition to thin-film structures such as CuInGaSe₂^{15,16} or CdTe¹⁵ cells, perovskite solar cells have grown significantly in the last 5 years.¹⁷⁻²¹ The latter developed from dye sensitized solar cells (DSSCs), which have recently experienced substantial developments as part of the new environmentally sustainable PV technologies after the appearance of a publication in *Nature* by O'Regan and Grätzel in 1991.²²⁻³¹

The organic material-based solar cell has three types, i.e., perovskite solar cells, polymer heterojunction solar cells, and DSSC.³² Among them perovskite solar cells give the highest efficiency; 23.3% efficiency was reached recently by a perovskite solar cell with single-junction layout.³³ But the perovskite solar cell is less stable against oxygen and humidity, and the difficult production process still makes it very difficult to market.^{34,35} Polymer solar cells often require an intricate procedure for the manufacture of their cells and are less effective (10%).³⁶ The fabrication of DSSCs is much simpler and its related PCE has increased by 7% to ~14%.³⁷⁻³⁹ In all lighting conditions, DSSCs provide an effective power output, including fluorescent and LED lighting. In the conditions of diffused or dim sunlight they can also function well. In these lighting conditions, however, silicon-based solar cells are not as efficient and are not very competitive.⁴⁰

The solar cell industry can currently be split into large terrestrial power production panel facilities and smaller portable electronic modules.⁴¹ DSSCs may be used in both fields but within the second

context they are more promising. They demonstrate excellent performance under indoor environment with an artificial light source compared to other solar cell technologies.⁴² This performance is essential for the development and manufacturing of indoor DSSCs different applications. For example, the Internet of Things (IoT) is attracting global scientific and technological attention nowadays since it underlines connections among wireless sensor nodes, consumer electronic devices, wearable devices, and smart meters.^{43,44} Although many small devices are connected with communication networks, there are major issues with charging such devices.⁴⁴ For IoT devices, batteries may be used as power sources. However, the downside of the main batteries is that their lifespan is restricted within months to years. Such batteries need charging often for the secondary batteries. These issues do not occur in DSSCs, since the cells turn the room light directly into electricity without external power supply. In addition, the power needed for IoT devices is typically low and can be supplied under room light conditions by running the DSSCs. Hence, indoor DSSCs are regarded as promising IoT system power supply cells.⁴⁵

DSSC efficiency depends on various variables, such as system design, a spectral response module, nature of the active material, light source power intensity and illuminance, irradiance, reflection, and temperature. Figure 1 provides a schematic diagram illustrating these variables. Researchers have made considerable efforts over the last few years to improve cost-effective, robust and effective DSSCs for indoor applications; however, these attempts are still inadequate and their physical and chemical properties must be refined in order to increase the performance of DSSC and commercialization.^{46,47} Additional study is needed to address certain crucial DSSC issues such as environmental durability, lifespan, large-scale processing, mechanical efficiency and spectral compatibility between the active DSSC material absorption range and the indoor irradiance range of light sources. In this regard, a thorough analysis of the production of DSSC for indoor applications will be very helpful in exploring the different issues that need careful attention. Thus, in this review we focused on different anode, sensitizer, electrolyte, and cathode materials used for indoor DSSC with the hope that this review will offer guidance to young researchers on the potential development of new materials with improved efficiency. This review aims to bind the work of different researchers together in order to increase the efficiency of the DSSC for indoor applications. The suggested modifications and

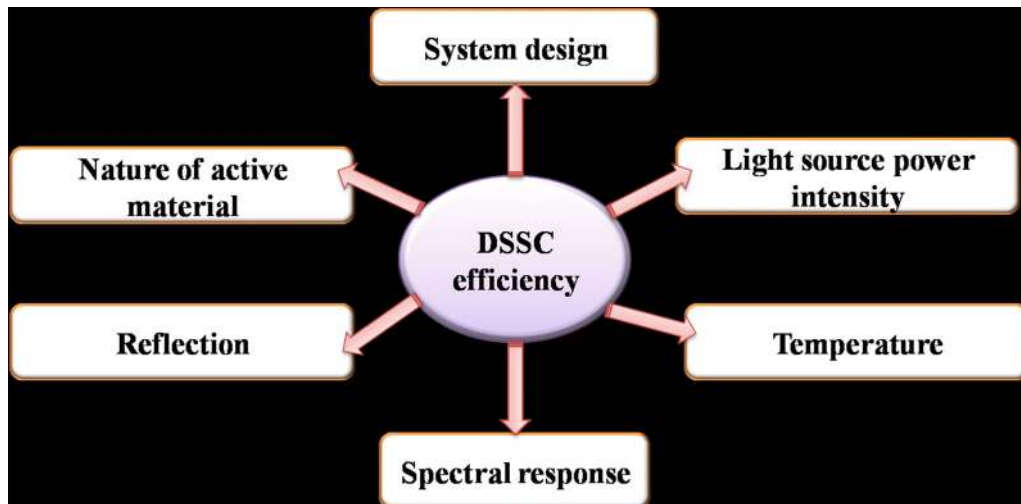


Fig. 1.. Illustration of the factors affecting efficiency of DSSC

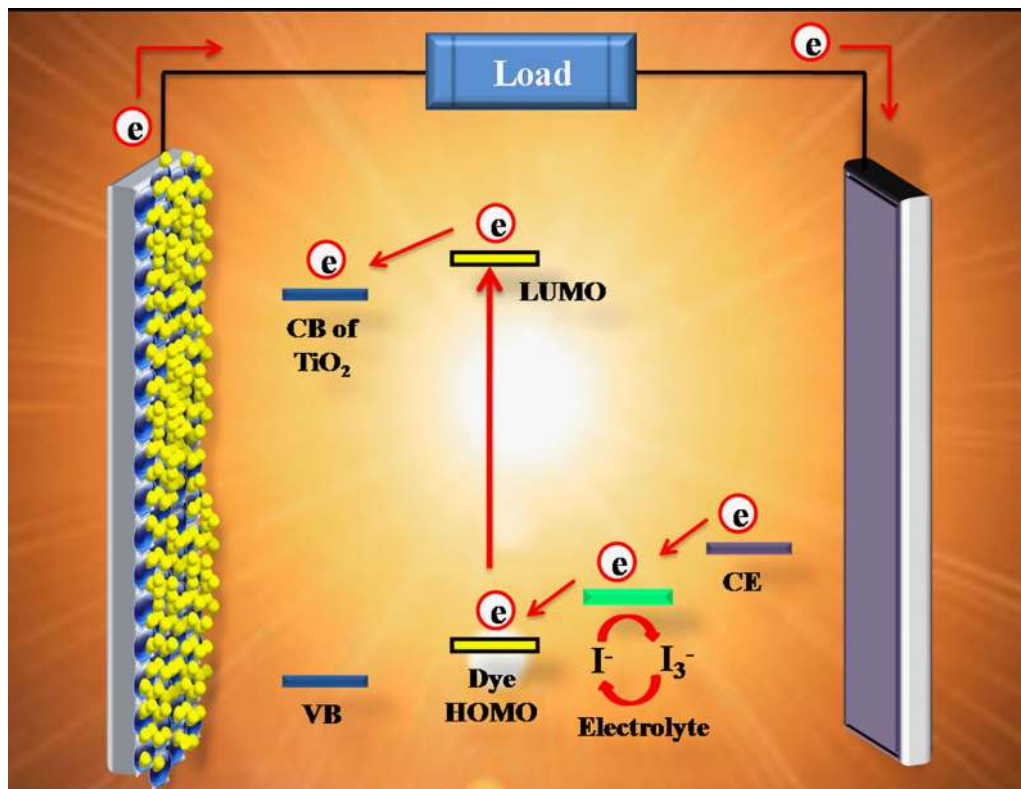


Fig. 2.. Working principle of DSSC

experiments are bifurcated appropriately, depending on the various DSSC components.

ARCHITECTURE OF DSSC

A standard DSSC consists of four essential components for initiating the conversion of solar energy to electrical energy.^{48–52} The components and their roles are: (i) photosensitizer for electron injection, (ii) photoanode for charge separation/conduction,

(iii) redox electrolyte for dye regeneration and (iv) counter electrode (CE) for electron collection, as displayed in Fig 2. Visible-light transmission (400–700 nm) of glass substrate coated with fluorine-doped tin oxide (FTO) or indium tin oxide (ITO) should be $> 80\%$ with low resistance (< 15 to $40 \Omega/\text{sq cm}$), allowing injection of electron and transmission. For superior conduction and transfer of charges, crystallization and annealing of titanium dioxide (TiO_2) film at $100\text{--}500^\circ\text{C}$ is necessary.

Covalently bound monolayer sensitizer molecules to the TiO₂ surface boost the absorption of photons and the production of e-h pairs. Regeneration of dye happens by solid (gel) or liquid electrolyte when sensitizers obtain their lost electrons from redox mediator reduction.

WORKING OF DSSC

The full operating process of DSSCs consists of the following phases.^{53–57}

- (i) Excitation of sensitizer (absorption of photonic energy): When sunlight strikes the DSSC, the sensitizer gets excited to a higher energy state [lowest unoccupied molecular orbital (LUMO)] from their ground state [highest occupied molecular orbital (HOMO)] and subsequently produces electrons and holes.
- (ii) Injection of electron: The excited sensitizer is oxidized and an electron is inserted into the conduction band (CB) of the semiconductor (TiO₂), whereby electrons pass through the thin film of porous TiO₂ to the transparent conducting oxide glass substrate to cathode from the anode through an external loop, creating current and completing cycles.
- (iii) Regeneration of sensitizer: The redox pairs present in the electrolyte (e.g. iodide and triiodide [I⁻ = I₃⁻] redox pairs) donate the electron to oxidized-sensitizer, and thus it gets regenerated.
- (iv) Electrochemical reduction: In addition, iodide and the redox mediator in the electrolyte travel to the CE and are regenerated on the cathode by reducing tri-iodide.

In DSSCs, two recombinant mechanisms may be taken into account, where the oxidation of sensitizing molecules and redox electrolyte species occurs in two competing chemical reactions simultaneously.⁵⁸ Within a microsecond timescale (10⁻⁶ s), the recombination of photogenerated electrons are takes place with redox species (I₃⁻) or/and oxidized sensitizers.^{59,60}

DSSC PERFORMANCE PARAMETERS

Since all forms of DSSCs are characterized by standard equipment for solar-cell testing, it is important to incorporate main parameters used for the experimental validation of DSSC systems.

An essential quantity reflecting a solar cell's total efficiency is the power conversion efficiency (PCE) (η):

$$\eta = \frac{V_{OC}J_{SC}FF}{P_{in}} \times 100\% \quad (1)$$

V_{OC} is the open-circuit voltage that is in contrast with the Fermi level of TiO₂ and the redox potential of the electrolyte,⁴² and the incident-light power density is P_{in} . J_{SC} is the current width of the short circuit. FF is the fill factor that demonstrates the cell's inherent quality.

$$FF = \frac{V_{max}J_{max}}{V_{OC}J_{SC}} \quad (2)$$

where V_{max} and J_{max} correspond to voltage (V) and current density (J) values that maximize their product.

RECENT DEVELOPMENT IN THE PHOTOANODE MATERIALS

Semiconducting metal oxides with a wide band gap were deposited on FTO or ITO and were used as photoanode materials. The recent advancement in materials used for the photoanode is presented here.

A thin layer of Nb₂O₅ was coated onto the FTO glass utilizing a simple dip-coating process as an effective DSSC photoanode substrate material and its blocking effect on the recombination of charges under different illuminance was analysed by Chen et al.⁶¹ The results showed that the blocking effect by Nb₂O₅ is strongly dependent on the illuminance intensity, whereas at strong (one sun, > 100,000 lux) illumination, the blocking effect of Nb₂O₅ is negligible, since the suppressed reverse charge flux allows no significant impact to high-level injection of photo-excited charges. In comparison, the blocking effect plays an essential role in increasing the performance as the photon-injected charge flux decreases dramatically at low-intensity illumination (300–6000 lux). Moreover the device showed a significant improvement in FF which successfully increased the PCE of DSSCs by 10% to 53% under low-intensity illumination from 6000 to 300 lux. Furthermore, the same research group⁶² deposited Nb₂O₅ above the TiO₂ layer via dip-coating with different cycles (1, 3 and 5). Results revealed that under one sun illumination, the device without Nb₂O₅ displayed an efficiency of 5.26% and the device with Nb₂O₅ (1 dipping cycle) displayed an efficiency of 5.94%. Also, the device with Nb₂O₅ showed the highest efficiency of 17.40% under 6000 lux illumination, whereas the device without Nb₂O₅ displayed 15.53% efficiency under the same condition. It suggests that the thin film of Nb₂O₅ serves as a shielding film which efficiently inhibits the recombination of charges on the photoanode.

Chou et al.⁶³ prepared a photoanode containing a composite of TiO₂-reduced graphene oxide–indium gallium zinc oxide (TGI), which was synthesized using a hydrothermal process, spin coating and sputtering. Their study revealed that the device with TGI photoanode displayed an efficiency of 5.66% and the device with TiO₂ displayed a PCE of 3.46% under 100 mW cm⁻² illumination, whereas

under 0.63 mW cm^{-2} illumination, both devices showed an increase in efficiency of 7.97% (TGI) and 4.70% (TiO_2). The highest efficiency of TGI based device was due to the reduction in dark reaction. RGO's intense electrical mobility speeds up photogenerated electrons from the TiO_2 conductive band to the FTO conductive band prior to recombination. In fact, the IGZO creates a shield to prevent the recombination of photogenerated electrons and I_3^- .

In one more work, Hora et al.⁶⁴ optimized the TiO_2 photoanode for DSSC's indoor application. In this work, photoanode mesoporous layers were modified in thickness and light-scattering capacity to optimize light harvesting and decrease recombination loss. A TiO_2 blocking layer and the TiO_2 mesoporous layer treated with titanium tetrachloride (TiCl_4) decreased the re-combination of the electron back with electrolyte. After the optimization, the device displayed 9.84% efficiency under simulated solar light and also it displayed 28.7% efficiency under indoor light condition.

For the activity of cobalt-mediated DSSCs under indoor light illuminations, compact blocking layer with powerful blocking feature is eminently necessary. The DSSCs use conventional TiCl_4 -derived blocking layers functions effectively under normal sunlight while the extreme transfer of electrons from the FTO to the electrolyte under room light condition limits the efficiency of these devices. To overcome this effect, Liu et al.⁶⁵ employed spray pyrolysis to prepare compact blocking layers. Their experimental finding shows that the compact blocking layer will prevent electron leakage across a broad spectrum of intensities, allowing the DSSCs to function efficiently in low-light conditions. Also, they anticipated that other methods of thin film production will perform a specific blocking role in addition to the spray pyrolysis. The device with compact blocking layer displayed highest efficiencies of 15.26%, 14.59%, and 15.12% compared to TiCl_4 blocking layer based DSSC (8.56%, 7.46%, and 6.19%) under 1001 lux, 601 lux, and 251 lux illumination, respectively.

Nien et al.⁶⁶ prepared TiO_2 nanofibers containing silver (Ag) NPs (TNSN) by employing the sol-gel method for photoanode application in DSSC. They prepared TNSN in two ways, firstly, they mixed TNSN with pristine TiO_2 and next, they initially coated pristine TiO_2 after which they coated TNSN above the TiO_2 layer (TiO_2/TNSN). Among these two photoanodes, the TiO_2/TNSN based device displayed the highest PCE of 5.13% under 100 mW cm^{-2} illumination. This was attributed to the inhibition of electron recombination by introducing the TNSN and the effective use of light radiation. Because of Ag's excellent conductivity, the electrons were transferred easily and the recombination of electrons was minimized. In comparison, the DSSC based on TiO_2/TNSN displayed an increase in efficiency of 6.23% under 30 mW cm^{-2} ; conversely,

its PCE reduced to 5.31% as light dropped to 10 mW cm^{-2} intensity.

A bifacial DSSC with improved light scattering was fabricated by Sasidharan et al.⁶⁷ by using templated TiO_2 surfaces formed by fugitive ZnO microflower inclusions. The optimized device showed highest efficiency of 6.82% and 4.71% under one sun condition front and back side illuminations, respectively. Further, it showed the highest efficiency of 11.8% under 1000 lux CFL illumination compared to bare TiO_2 (6.39%).

RECENT DEVELOPMENTS IN THE ELECTROLYTE MATERIALS

Typically, DSSCs with novel sensitizers and iodide electrolyte are used in room light applications.⁶⁸⁻⁷¹ The optimal conditions used for these devices vary from those which work under AM 1.5 solar light conditions. Unlike AM 1.5 solar light conditions, under indoor light conditions only a few electrons are excited. These electrons are easily recombined with the redox pairs, which has a serious effect on the cell V_{OC} .⁷² Similarly, under room light illumination, the formation of excited holes reduce, under which a limited volume of iodide is adequate to minimize the number of holes created. Because of the amount of iodine in the electrolyte, the light intensity is often influenced. To overcome this problem, Venkatesan et al.⁷³ prepared an electrolyte using a cobalt redox pair and 3-methoxypropionitrile solvent. Also, they regulated the DSSC components, photoanode, CE, and electrolytes to get the finest device performance. The experimental findings reveal that the DSSC with a photoanode with a TiO_2 layer that is $10 \mu\text{m}$ thick ($4 \mu\text{m}$ scattering layer and $6 \mu\text{m}$ main layer), Y123 dye, an electrolyte consisting of a Co (II / III) ratio of 0.11/0.025 M, 1.2 M 4-tert-butylpyridine, a CE with a Pt layer thickness of 0.16 nm are the ideal conditions for obtaining a high PCE. This device displayed the highest efficiency of 24.52%, 23.48%, and 22.66% under T5 light illumination of 999.6 lux, 607.8 lux, and 201.8 lux. At a TiO_2 layer of $8 \mu\text{m}$ thickness, the bifacial cell demonstrated an optimum PCE of 17.31% under rear illumination and 20.65% under front illumination. Moreover, these devices were also long-lasting and were able to maintain 100% of their initial performance after a 1000-h examination at 35°C .

To date, the efficiency of liquid-state devices under ambient light conditions has only been recorded by minimal studies. The key concern of this DSSC class is electrolyte leakage and organic solvent evaporation. This disadvantage greatly affects the DSSCs' long-term performance, which can limit their IoT applications and other applications. In comparison, good efficiency was only obtained in laboratory devices using the injection technology for fabrication. In reality, this approach is not ideal for large-scale cells. The

printable electrolytes (PEs) can solve these two issues, which can be coated using a printing technique on a photoelectrode.^{74–77} This method can be used in large-scale DSSC development due to good penetration of the extremely viscous polymer gel electrolytes and roll-to-roll coating processes. Venkatesan et al.⁷⁸ have developed printable electrolytes for this reason, using 3-methoxypropionitrile comprising TiO₂ nanofillers, polyethylene oxide (PEO)/polyvinylidene fluoride (PVDF) gelator, and an iodide/tri-iodide redox mediator. They observed that modifying the formulations of the polymers did not significantly affect the PCE of the DSSCs. The device efficiency relied mainly on the TiO₂ thickness in the photoelectrode and the concentration of the iodine in the electrolyte. The diffusivity of ions reduced and the conductivity of electrolytes improved with an increased concentration of iodine in the electrolyte. Nevertheless, the DSSC's efficiency was not linked to the electrolytes ion conductivity and diffusivity characteristics, but instead to the photoelectrode/electrolyte interface charge transfer resistance and the DSSC's IPCE. Furthermore, the optimized device having N719 dye displayed the highest efficiency of 20.67% and 15.39% under 600 lux and 200 lux illumination, respectively. In addition, high efficiencies of 12.8% and 11.2% were achieved by the sub-module cells using Z907 and N719 sensitizers, respectively, under 200 lux irradiation. The long-term stability analysis reveals that after 1000 h of under 200 lux irradiation, the production of DSSC would maintain its initial performance by 97%.

In one more work, the same research group⁴⁵ prepared cobalt based gel polymer electrolyte (GPE) containing poly(vinylidene fluoride-co-hexafluoropropylene) and different metal oxide nanofillers for DSSC indoor application. Among the other GPE, zinc oxide nanofillers containing GPE displayed the highest efficiency of 20.11% under 200 lux of T5 fluorescent light which is higher than the corresponding liquid-state DSSC. Where, zinc oxide nanofillers reduce the diffusivity of ions and the electrolytes conductivity. However, the efficiency of the device was not affected by this, but were highly reliant on the DSSC capacitance and charge transfer resistance at the photoelectrode/electrolyte interface, whereas the reduction in capacitance and the rise in charge transfer resistance at the photoelectrode/electrolyte interface in the zinc oxide nanofillers's presence contributed to the DSSC's high V_{OC} . Furthermore, the iodine or cobalt redox couple containing PEO and poly(methyl methacrylate) (PMMA) PEs were prepared by the same research group.⁷⁹ Moreover, PEO PE with a cobalt redox mediator has shown to be more ideal for assembly of high-performance room light DSSCs (21.06%) than iodide PEO/PMMA PE. The optimum PEO PE had less ion conductivity and diffusivity than the respective liquid electrolyte. The efficiency

of the DSSC with this PE was, however, close to that of the device utilizing liquid electrolyte under the illumination of 200 lux T5 radiation. Also, this efficiency was considerably superior to the DSSC efficiency using iodide PEs. The cobalt PE sub-modulated cell displayed a high efficiency of 12.60%, whereas the bifacial DSSCs utilizing the 9 wt% PEO demonstrated a performance of 17.60% and 14.58% under the 200 lux conditions from front and back illumination, respectively. These PE-based cells showed greater stability than the liquid electrolyte-based cells at 35 °C.

Double-layered printable electrolytes were prepared by Liu et al.⁸⁰ using PVDF and PEO blend having zinc oxide. The optimized device showed the highest efficiency of 8.50%, 15.7%, and 15.9% under AM 1.5G, indoor fluorescent lighting 200 lux and 1000 lux conditions, respectively.

RECENT DEVELOPMENTS IN THE CE MATERIALS

The CE, a major component of a DSSC, must have a high conductivity to transport electrons flowing via an external circuit and an excellent catalytic ability to reduce I₃⁻.^{81–84} Pt is the most frequently used catalyst on the CE in DSSCs because of its high stability, high conductivity and high electrocatalytic activity towards redox reaction. But the Pt CE's high cost and energy-consuming manufacturing process restricts its applicability. To replace Pt-based CE, a CoSe₂/CoSeO₃ hierarchical urchin-like structured (CoSe₂/CoSeO₃-UL) CE material was prepared by Huang et al.⁸⁵ via a one-step hydrothermal process. For comparison, they also prepared CoSe₂/CoSeO₃ nanoparticles and platinum (Pt)-based CEs. CoSe₂/CoSeO₃-UL comprises hexagonal prisms and nanoparticles which provide a one-dimensional charge transport route and a large surface area for catalytic reactions, respectively. Under 1 sun condition, a CoSe₂/CoSeO₃-UL CE based device displayed the highest efficiency of 9.29% compared to Pt (8.33%) and CoSe₂/CoSeO₃-NP (8.81%) CE based devices. Also, under dim light conditions, CoSe₂/CoSeO₃-UL CE based device showed efficiencies of 16% (4,800 lux), 18.24% (6,000 lux), and 19.88% (7,000 lux). Further, the same research group⁸⁶ also prepared pristine carbon aerogels (CAs) based CE for replacing Pt CE, whereas the CAs were prepared via sol-gel method by regulating the molar ratios of resorcinol (R)/sodium carbonate (C) and resorcinol (R)/formaldehyde (F). They found that highest specific surface area of the CE reached 724 m² g⁻¹ with 377 and 0.76 molar ratios of R/C and R/F and this CE based device displayed the highest efficiency of 9.08% under 1 sun condition. Also, this device achieved an efficiency of 9.16% and 20.1% under 0.5 sun and T5 lamp with 7000 lux conditions, respectively. In addition, CoSe₂/CoSeO₃-UL

and CAs have tremendous potential to substitute Pt in DSSCs as a highly effective electro-catalyst.

RECENT DEVELOPMENTS IN THE SENSITIZERS

Among the dyes developed (metal-free organic dyes, ruthenium, porphyrin, etc.), metal-free organic sensitizers have been studied extensively due to the benefits of low synthetic cost, versatile molecular design, environmental friendly and potentially higher extinction coefficients.^{87,88} Recently, ample work has been conducted to make all feasible improvements in the sensitizers for indoor DSSC applications. Few of those are presented here. The chemical structures of the dyes are presented in a separate section below and the corresponding PV parameters of DSSCs under room light conditions are presented in Table I.

Chen et al.⁸⁹ synthesized a sequence of dyes (**1-6**) for DSSCs and tested them under standard AM 1.5 and indoor light illuminations. Under AM 1.5 conditions, the highest efficiency was obtained for dye **4** based device (5.02%). While the highest efficiency values obtained under the T5 and LED lamps were 13.43% (dye **4**) and 12.21% (dye **6**), respectively. They explored the connection between the dye's molecular structure and their subsequent efficiency and they found the following approaches to produce the optimal sensitizers for indoor light condition. (i) It is desirable to increase the amount of alkyl chains on the sensitizers to lift the V_{OC} of the device. (ii) The dye's absorption range would also align with the indoor light emission spectra. The emission spectrum of indoor light does not cover the near-infrared region (NIR) region (> 700 nm) as opposed to the solar spectrum. For this case, the optimal dye under indoor lighting does not require either a long conjugation framework or a strong dipole, which dramatically lowers the synthetic costs of the dyes.

Furthermore, four new dyes (**7-10**) with two bis(alkoxy)phenyl substituent containing a benzo[3,4-b]pyrazine (BP) or a thieno[3,4-b]pyrazines (TP) agent as auxiliary acceptor were reported by Desta et al.⁹⁰ They found that the addition of the 3,4-dihexyloxyphenyl moiety at the TP and BP's 2- and 3-sites increases its solubility in organic solvents and helps inhibit dark current in the device. The devices produced from the two BP dyes (**8** and **10**) with a chenodeoxycholic acid displayed efficiency of 8.39% and 9.03% respectively, under 1 sun

illumination. Also, **10** exhibited a PCE of 27.17% and 18.95% under 6,000 lux and 300 lux luminance, respectively, under dim light conditions.

For indoor and outdoor dye-sensitized studies of solar cells, three novel organic dyes based on anthracene, denoted as **11**, **12**, and **13** were synthesized by Tsai et al.⁹¹ Further, they prepared flexible and rigid modules, as well as small cells, and their PV efficiencies were evaluated. The **11** unit gives rise to a black colour and exhibits an excellent PV efficiency, because of the panchromatic absorption of visible light. Under 1000 lux fluorescent light of T5, the **11/R26** module performs better than the Z907 counterpart with an efficiency of 11.94%. Furthermore the same research group⁹² synthesized five more dyes labeled **14**, **15**, **16**, **17**, and **18**. **15**, **14**, and **11**, (or **18**, **17** and **16**) chemical structures vary in their anchoring groups, i.e., hydroxamic acid, isophthalic acid, and carboxylic acid, respectively. Additionally, an ethynyl bridge is positioned between the anchoring groups and the benzothiodiazoyl moiety for **16**, **17**, and **18**. The small cell with **16** outperforms others and the counterpart (dye **11**) under 1 sun irradiation. Further, under 1000 lux of indoor light T5, the **16** based device displayed PCE of 13.48% which surpasses the PCE of the **11** based device (11.94%).

Chou et al.⁹³ synthesized perylene based dyes (**19-23**) with N,N-diarylamine and arylcarboxylic acid as the donor and acceptor units, respectively. The **23** dye displayed the highest efficiency of 6.16% using liquid iodide-based electrolyte under the illumination of AM 1.5 G simulated sunlight. This dye based device also showed a good efficiency of 15.79% under 6000 lux light intensity (T5). Ironically, under the same condition, **19** with a simple molecular structure showed an efficiency of 15.01%.

Freitag et al.⁴² fabricated a device with two sensitizers (**24** and **25**) with Cu(II/I)(tmby) redox couple (tmby = 4,4',6,6'-tetramethyl-2,2'-bipyridine). The optimized device displayed a V_{OC} over 1 V and high efficiency of 11.3%. Also, this device reached an external quantum efficiency for photocurrent generation that surpassed 90% over the entire visible domain from 400 to 650 nm and achieved power outputs of 15.6 mW cm⁻² (200 lux) and 88.5 mW cm⁻² (1000 lux). Under 1000 lux condition, the optimized device showed the highest PCE of 28.9%.

A series of dyes (**26-31**) with spiro[fluorene-9,9'-phenanthren]-1"-one as an auxiliary acceptor were

Table I. PV parameters of different dyes based DSSC under room light conditions.

Dyes	PCE (%)	FF	V _{OC} (V)	J _{SC} (mA/cm ²)	Light source	Light intensity (lux)	References	
1	6.42	0.67	0.5	0.038	LED	600	89	
	7.8	0.67	0.49	0.044	T5	600		
2	11.71	0.73	0.57	0.056	LED	600		
	12.73	0.71	0.55	0.06	T5	600		
3	6.56	0.69	0.53	0.036	LED	600		
	9.99	0.71	0.55	0.047	T5	600		
4	11.49	0.7	0.58	0.056	LED	600		
	13.43	0.7	0.6	0.058	T5	600		
5	10.76	0.73	0.59	0.050	LED	600		
	12	0.71	0.6	0.053	T5	600		
6	12.21	0.71	0.56	0.061	LED	600		
	12.74	0.7	0.5	0.062	T5	600		
7+CDCA	6.39	0.75	0.49	0.015	T5	300	90	
	6.67	0.75	0.51	0.029	T5	600		
	6.81	0.76	0.53	0.044	T5	900		
	8.62	0.76	0.58	0.315	T5	6000		
8+CDCA	15.1	0.77	0.54	0.033	T5	300		
	16.49	0.77	0.68	0.067	T5	600		
	17.38	0.78	0.58	0.104	T5	900		
	23.17	0.79	0.65	0.762	T5	6000		
9+CDCA	12.08	0.76	0.54	0.26	T5	300		
	12.79	0.77	0.56	0.53	T5	600		
	13.24	0.77	0.57	0.8	T5	900		
	16.86	0.77	0.63	0.562	T5	6000		
10+CDCA	18.95	0.75	0.57	0.04	T5	300		
	20.16	0.76	0.59	0.081	T5	600		
	21.1	0.76	0.61	0.124	T5	900		
	27.17	0.76	0.67	0.913	T5	6000		
11	9.08	0.64	0.90	0.010	T5	200	91	
	11.17	0.65	1	0.034	T5	600		
	11.94	0.64	1.05	0.061	T5	1000		
	9.68	0.64	0.9	0.010	LED	200		
	10.95	0.65	0.99	0.031	LED	600		
	11.26	0.64	1.03	0.529	LED	1000		
16	11.77	0.68	0.43	0.023	T5	200		92
	13.30	0.70	0.47	0.066	T5	600		
	13.48	0.75	0.49	0.116	T5	1000		
	9.13	0.66	0.42	0.021	LED	200		
	11.29	0.7	0.47	0.064	LED	600		
	12.82	0.75	0.49	0.114	LED	1000		
19+CDCA	9.15	0.69	0.49	0.027	T5	300	93	
	10.37	0.72	0.50	0.056	T5	600		
	11.27	0.73	0.51	0.085	T5	900		
	12.14	0.73	0.53	0.117	T5	1200		
	12.94	0.74	0.55	0.221	T5	2400		
	13.49	0.74	0.57	0.334	T5	3600		
	14.19	0.74	0.58	0.459	T5	4800		
	15.01	0.74	0.59	0.594	T5	6000		
	8.35	0.70	0.46	0.026	LED	350		
	9.29	0.72	0.49	0.048	LED	600		
	10.47	0.72	0.51	0.076	LED	900		
	10.74	0.73	0.52	0.102	LED	1200		
	12.13	0.74	0.56	0.213	LED	2400		
	12.56	0.74	0.57	0.321	LED	3600		
	12.62	0.74	0.58	0.427	LED	4800		
	13.05	0.74	0.59	0.540	LED	6000		

Table I. continued

Dyes	PCE (%)	FF	V _{OC} (V)	J _{SC} (mA/cm ²)	Light source	Light intensity (lux)	References
23+CDCA	9.12	0.62	0.45	0.029	T5	300	93
	11.76	0.68	0.48	0.062	T5	600	
	12.24	0.70	0.49	0.093	T5	900	
	13.26	0.72	0.50	0.127	T5	1200	
	14.12	0.74	0.53	0.254	T5	2400	
	14.83	0.75	0.54	0.382	T5	3600	
	15.29	0.75	0.55	0.510	T5	4800	
	15.79	0.76	0.56	0.640	T5	6000	
	8.13	0.63	0.45	0.029	LED	350	
	9.58	0.68	0.48	0.053	LED	600	
	10.29	0.70	0.49	0.080	LED	900	
	11.08	0.72	0.51	0.109	LED	1200	
	12.11	0.74	0.53	0.222	LED	2400	
	12.57	0.75	0.54	0.334	LED	3600	
	13.03	0.76	0.56	0.443	LED	4800	
13.10	0.76	0.56	0.557	LED	6000		
24:25	25.5	0.79	0.73	0.027	Osram warm white 930	200	42
	28.9	0.8	0.79	0.138		1000	
26	16.64	0.70	0.55	0.078	TL84	1000	94
	17.94	0.71	0.59	0.195	TL84	2500	
27	8.23	0.58	0.57	0.045	TL84	1000	
	9.02	0.61	0.61	0.110	TL84	2500	
28	18.15	0.66	0.59	0.085	TL84	1000	
	20.83	0.68	0.63	0.222	TL84	2500	
29	10.03	0.58	0.57	0.05	TL84	1000	
	11.76	0.59	0.63	0.146	TL84	2500	
30	16.94	0.65	0.59	0.08	TL84	1000	
	19.74	0.69	0.65	0.201	TL84	2500	
31	9.36	0.56	0.58	0.051	TL84	1000	
	11.74	0.60	0.65	0.137	TL84	2500	
N719:28	24.45	0.66	0.569	0.12	TL84	1000	
	26.19	0.69	0.628	0.278	TL84	2,500	
32	4.43	0.55	0.405	0.021	TL84	600	26
	7.50	0.83	0.415	0.040	TL84	1000	
	7.72	0.64	0.462	0.120	TL84	2500	
33	6.71	0.58	0.459	0.030	TL84	600	
	8.52	0.71	0.459	0.048	TL84	1000	
	9.03	0.65	0.481	0.133	TL84	2500	
34	7.35	0.60	0.427	0.031	TL84	600	
	9.64	0.62	0.436	0.065	TL84	1000	
	9.86	0.70	0.492	0.131	TL84	2500	
35	10.16	0.61	0.417	0.044	TL84	600	
	11.07	0.58	0.444	0.078	TL84	1000	
	12.14	0.66	0.496	0.170	TL84	2500	
36	12.38	0.55	0.480	0.052	TL84	600	
	18.99	0.67	0.550	0.095	TL84	1000	
	19.89	0.65	0.570	0.248	TL84	2500	
37	24.37	0.64	0.555	0.075	TL84	600	
	27.58	0.7	0.570	0.128	TL84	1000	
	27.82	0.69	0.597	0.309	TL84	2500	
37+DCA	25.42	0.66	0.56	0.075	TL84	600	
	27.40	0.63	0.62	0.129	TL84	1000	
	28.95	0.70	0.62	0.303	TL84	2500	
37:34	27.76	0.67	0.537	0.084	TL84	600	
	28.74	0.64	0.598	0.137	TL84	1000	
	30.45	0.72	0.621	0.312	TL84	2,500	

Table I. continued

Dyes	PCE (%)	FF	V _{OC} (V)	J _{SC} (mA/cm ²)	Light source	Light intensity (lux)	References		
39	15.6	0.51	0.487	0.038	T5	187	95		
	17.2	0.57	0.523	0.111	T5	597			
	12.4	0.56	0.542	0.133	T5	1025			
40	18.7	0.55	0.495	0.041	T5	187			
	18.6	0.58	0.525	0.115	T5	597			
	15.6	0.65	0.552	0.143	T5	1025			
41	22	0.58	0.501	0.045	T5	187			
	23.6	0.61	0.528	0.138	T5	597			
	21.4	0.65	0.556	0.156	T5	1025			
41+CDCA	27.5	0.59	0.526	0.053	T5	187			
	26.8	0.62	0.568	0.144	T5	597			
	25	0.63	0.576	0.224	T5	1025			
42	19.46	0.76	0.585	0.827	T5	6,000	96		
42:CW10	22.58	0.74	0.646	0.883	T5	6,000			
24:43	29.2	0.78	0.86	0.131	LED	1000	97		
46	18.76	0.73	0.57	0.038	T5	300	98		
	19.93	0.74	0.60	0.077	T5	600			
	21.85	0.74	0.62	0.121	T5	900			
	22.80	0.74	0.63	0.164	T5	1200			
	24.06	0.75	0.66	0.336	T5	2400			
	25.03	0.75	0.67	0.511	T5	3600			
	25.68	0.75	0.68	0.669	T5	4800			
	26.19	0.76	0.69	0.881	T5	6000			
	46+CDCA	21.4	0.76	0.62	0.039	T5		300	
		21.8	0.77	0.64	0.078	T5		600	
		23.6	0.77	0.66	0.121	T5		900	
46+CDCA	24.4	0.77	0.67	0.164	T5	1200			
	25.6	0.78	0.69	0.333	T5	2400			
	26.8	0.78	0.70	0.511	T5	3600			
	27.6	0.78	0.71	0.693	T5	4800			
	28.5	0.78	0.71	0.883	T5	6000			
	47+CDCA	2.48	0.68	0.50	0.061	D65		1000	99
		7.26	0.69	0.49	0.040	CWF		1000	
		8.12	0.69	0.52	0.092	CWF		2200	
		2.4	0.42	0.42	0.015	TL84		600	
		7.59	0.68	0.48	0.043	TL84		1000	
	51	8.78	0.69	0.53	0.111	TL84		2500	100
9.90		0.65	0.47	0.044	T5	600			
12.95		0.71	0.5	0.081	T5	1200			
14.68		0.7	0.53	0.15	T5	1800			
16.41		0.71	0.52	0.21	T5	2400			
17.02		0.7	0.55	0.24	T5	3000			
20.98		0.71	0.60	0.62	T5	6000			

CDCA= Chenodeoxycholic acid; DCA= Deoxycholic acid;

prepared by Huang et al.⁹⁴. The auxiliary moiety has the ability to reduce intermolecular accumulation and trap the I_3^- and Li^+ ions which prolongs the recombination of charges. Among the other dyes, the **28** based device (without deoxycholic acid) displayed the highest efficiency of 6.3% and 20.83% under AM 1.5 solar condition and TL85 (2500 lux) condition, respectively. Further, they measured the efficiency of DSSC with co-sensitization of **28** and N719 dyes. The optimized device displayed the highest efficiency of 8.55% under 1 sun illumination and also increased its efficiency to 24.45% and 26.19% at 1000 and 2500 lux illuminations, respectively. In addition, at 2500 lux condition, this device displayed a high stability that retained 84.5% after 336 h.

Dyes (**32-37**) with quinoxaline or quinoxalinoid moieties were synthesized by Jiang et al.²⁶ and studied their performance under room light and 1 sun conditions. Furthermore, the dyes with donor group at 2,3-positions of quinoxaline (**34** and **35**) displayed less PCEs compared to the donor unit at 5,8-positions (**36** and **37**). Under AM 1.5 solar light, **37** displayed the highest PCE of 6.96% when it was co-deposited with deoxycholic acid. They also found that the co-deposition of **34** and **37** enhances the coverage of the sensitizer on the TiO_2 surface which promotes the efficiency of the device to 7.92%. Under indoor illumination, also **37** with and without deoxycholic acid based devices displayed outstanding efficiencies. The **34** and **37** co-sensitized devices displayed the highest efficiency of 30.45% (2500 lux), under indoor light conditions.

Li et al.⁹⁵ reported **38-41** dyes with tetraphenylethylene substituted phenothiazine (at N-position) core with different π -bridges (4-heptyl-4-hexyl-4H-cyclopenta[2,1-b:3,4-b']dithiophene, 4-hexyl-2,2'-bithiophene, 3-hexylthiophene, or thiophene). These dyes built double-layered shelters to effectively prevent the oxidized electrolytes from reaching the TiO_2 surface and also improved their light harvesting property. Among the other dye based devices, **41**-based system displayed the highest PCE of 9.79% under simulated AM 1.5 G condition, beating that of the N719 sensitized system (8.77%). After the addition of the co-adsorbent chenodeoxycholic acid, the output improved to 10.87%. In comparison, the **41**-based DSSC demonstrated impressive efficiencies of 24.98%, 26.81%, and 27.54% at 1,025 lux, 597 lux, and 187 lux, respectively, under dim light conditions.

An anthracene based dye (**42**) having benzoic acid acceptor group was synthesized by Reddy et al.⁹⁶. The **42** dye based device showed an efficiency of

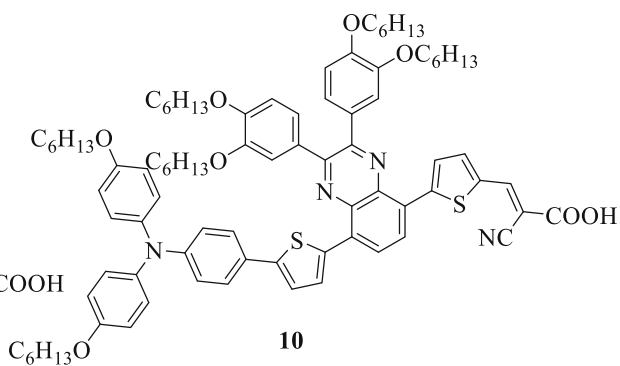
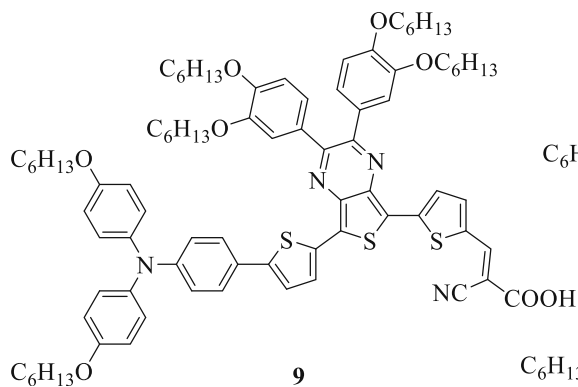
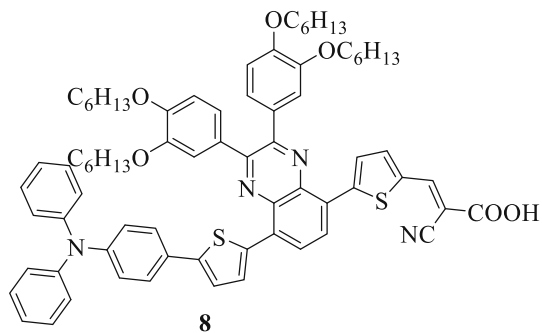
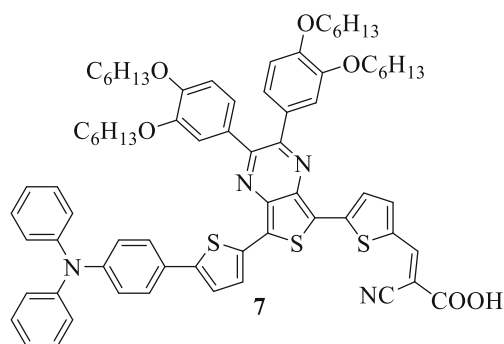
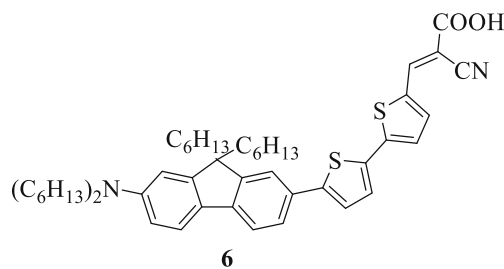
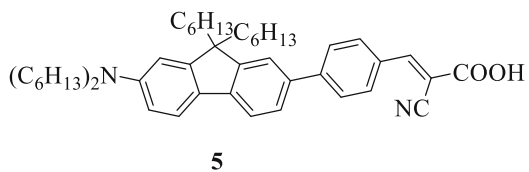
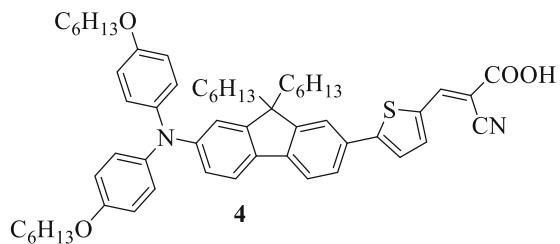
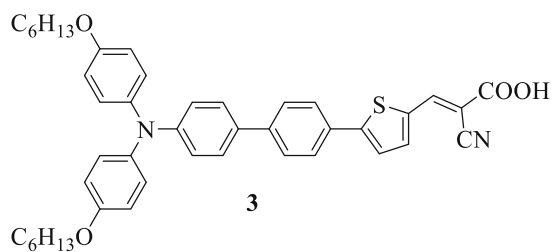
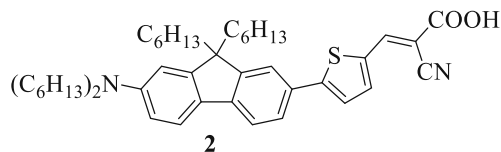
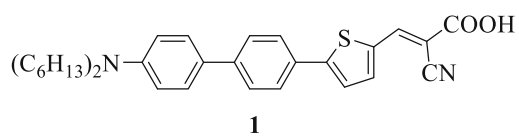
5.75% under AM 1.5G condition, whereas under low light illumination of 6000 lux, the efficiency was increased to 20.95%. In addition, they also co-sensitized **42** with porphyrin dye which displayed efficiencies of 6.31 and 22.58% under AM 1.5 G and 6000 lux illuminations respectively.

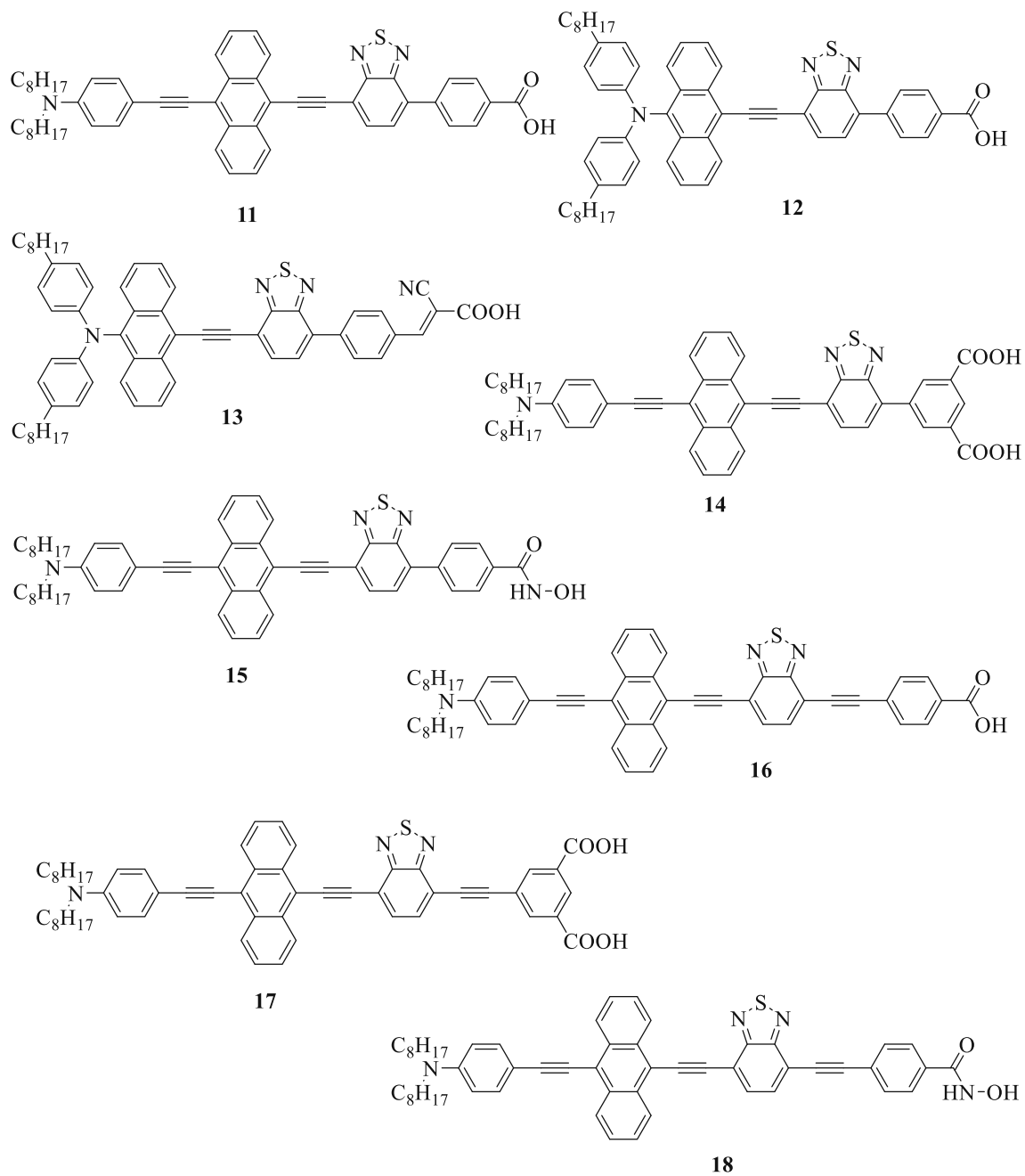
Tanaka et al.⁹⁷ co-sensitized **43** dye with **24** dye to attain an efficient DSSC and used the $Cu^{I/II}(tmby)_2$ electrolyte. Co-sensitized device displayed an efficiency of 9.1% at 1 sun and 9.4% at 0.1 sun conditions, superior or similar to the device utilizing **24** dye. Further, under artificial fluorescent lighting, the co-sensitized device displayed an efficiency of 29.2% at 1000 lux. They also mentioned that the cost of the sensitizer estimated to be decreased by ca. 30% if the **24** based device is replaced with the co-sensitized device without any loss of efficiency.

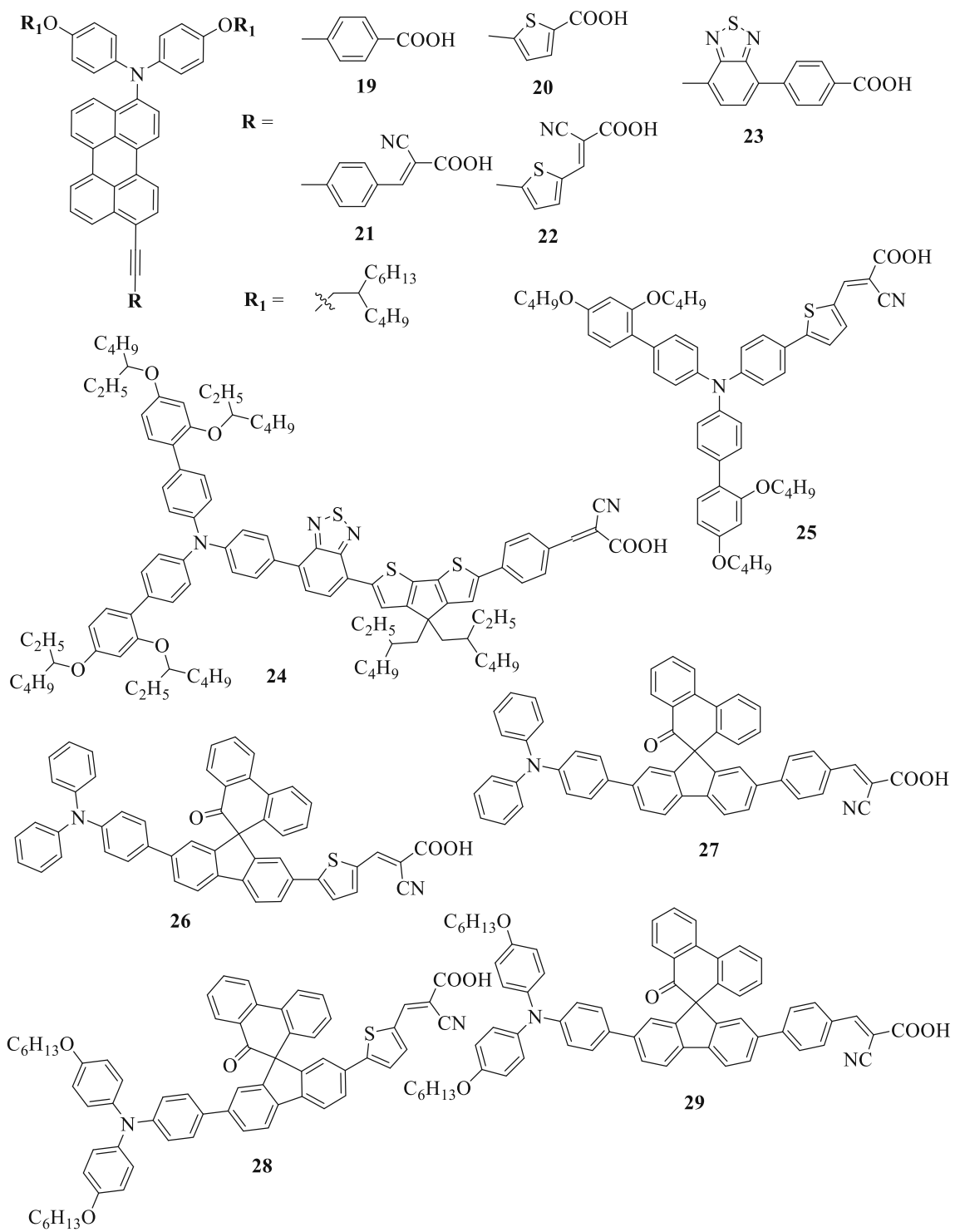
Tingare et al.⁹⁸ synthesized dyes (**44**, **45**, and **46**) using easy, convergent and short synthetic routes, suitable for large-scale manufacturing. Their analysis revealed that the modification of alkyl to alkoxy chain and the insertion of electron deficient molecules into the **44**, **45**, and **46** dyes played an important role in increasing their performance. When PCE of **46** based DSSC was measured under 1 sun conditions, it displayed the highest efficiency of 8.08% compared to other dyes. In fact, sensitizer **46** reached a PCE of 20.72% and 28.56% while measuring 6000 lux under the commercial light emitting diode light source and T5 fluorescent lighting, respectively.

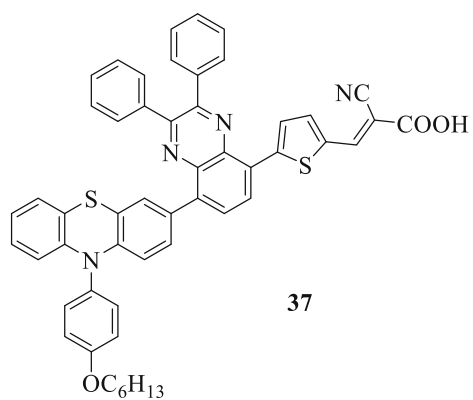
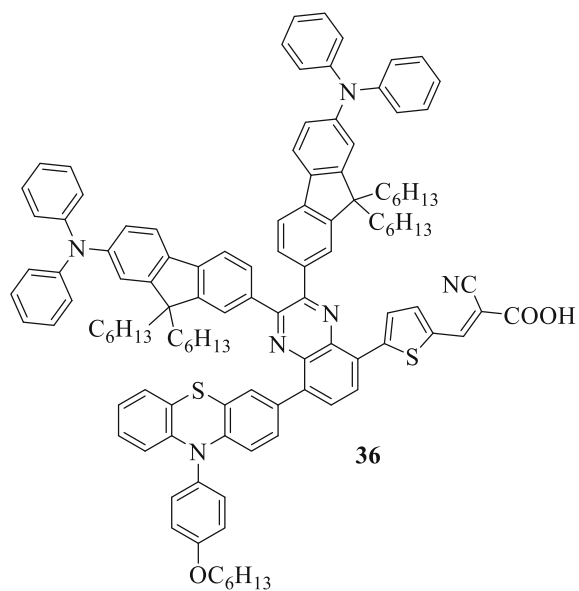
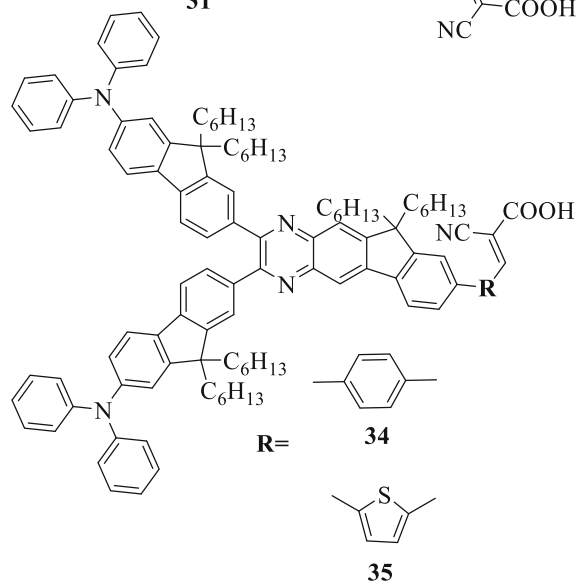
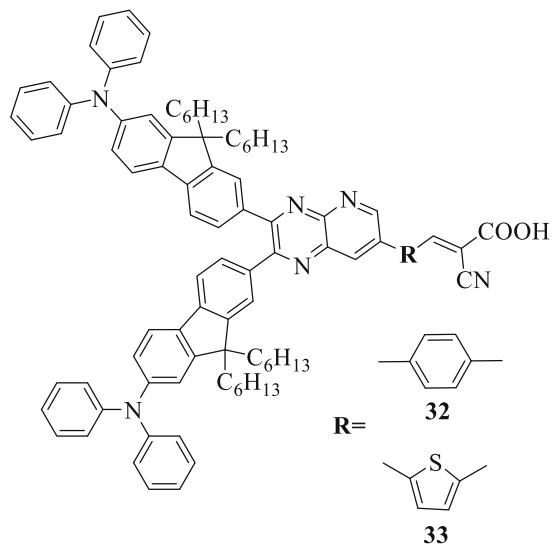
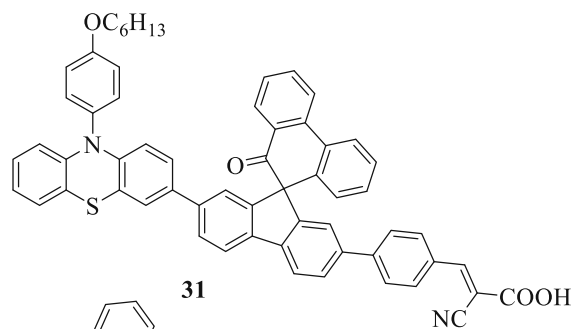
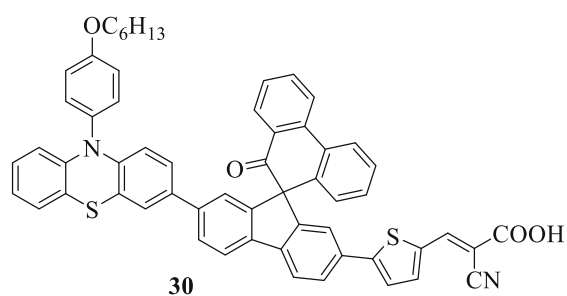
A series of sensitizers (**47-50**) containing T-shaped diarylamines as donors (phenyl-1-naphthylamine or diphenylamine), a dibenzofulvene connected to furanyl or thienyl as a π -spacer, and cyanoacrylic acid as anchoring units were synthesized by Chen et al.⁹⁹. The optimized **47**-based DSSC with co-adsorbent displayed the highest efficiency of 2.42%, FF of 0.63, a V_{OC} of 0.63 V, and J_{SC} of 6.01 $mA\ cm^{-2}$ under AM 1.5 condition. The same experiment was also carried out with respect to multiple light intensities such as TL84, CWF, and D65. As a consequence, the **47**-based device under 2500 lux intensity of TL84 showed the best efficiency of 8.78%.

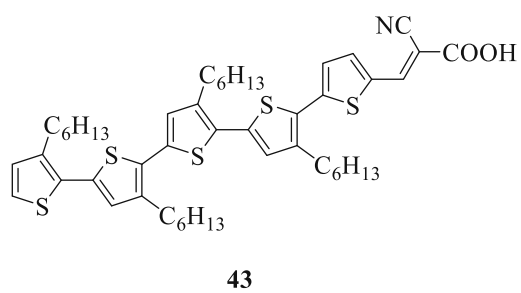
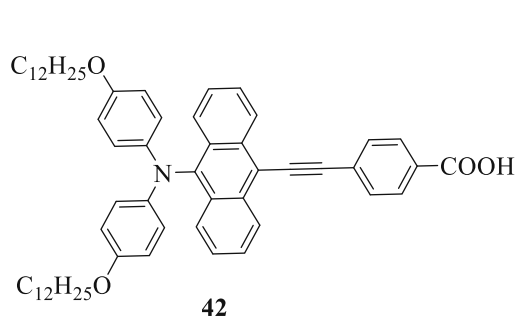
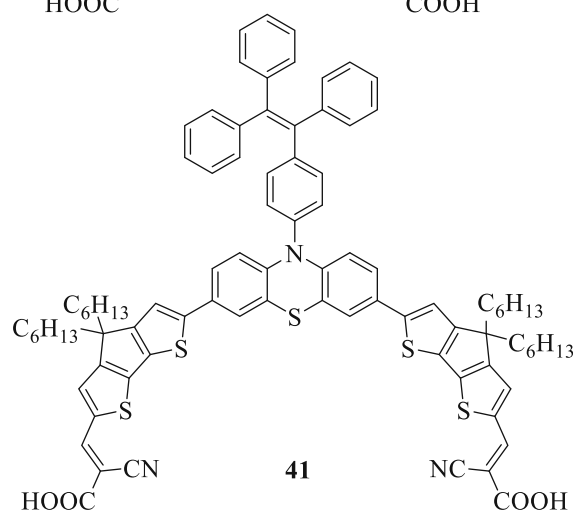
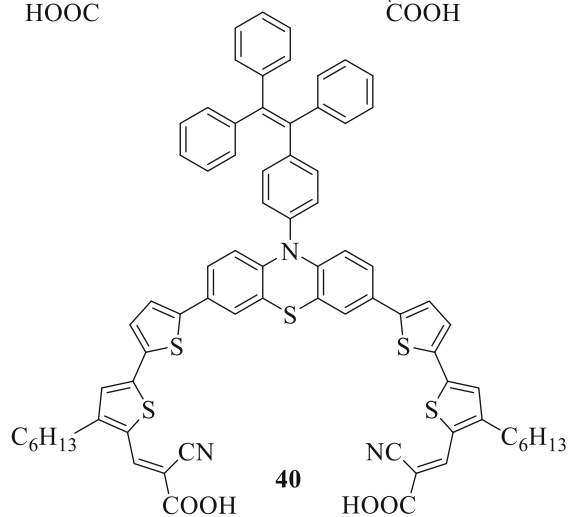
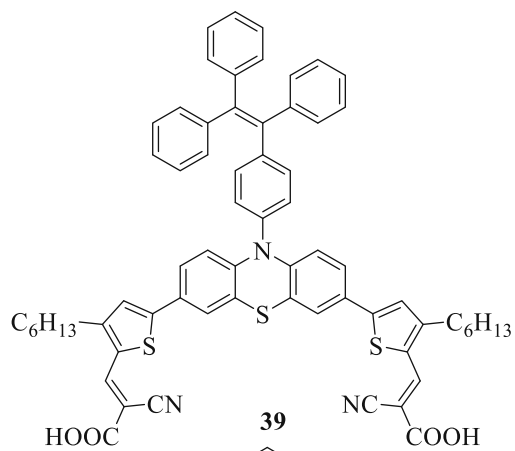
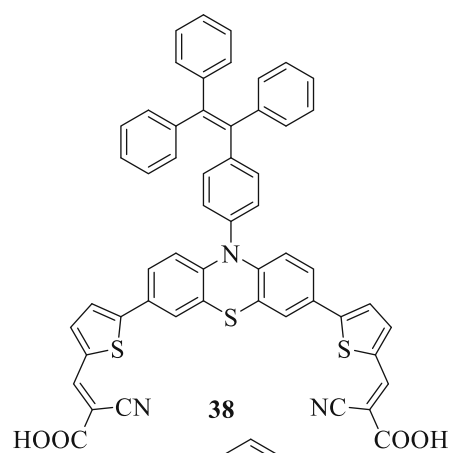
Sil et al.¹⁰⁰ fabricated DSSC by using dye **51** as sensitizer, PVP-Pt on ITO glass or sputter-Pt on ITO/PET based counter electrode and altering the thickness of TiO_2 layer. The optimized device having 8 μm thick TiO_2 layer, sensitized with **51** and PVP-Pt on ITO counter electrode showed the highest efficiency of 20.98% under 6000 lux illumination. At the same condition the efficiency of 19.69% was exhibited by the N719 dye sensitized device.

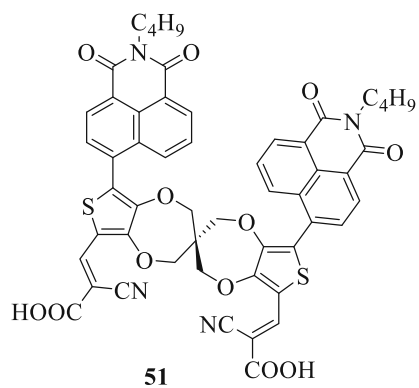
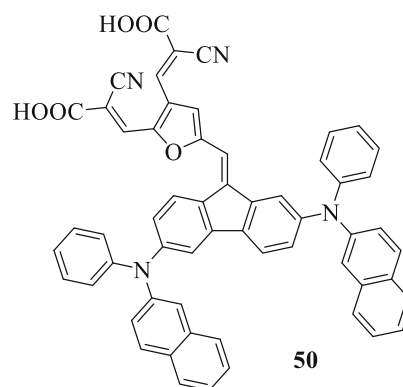
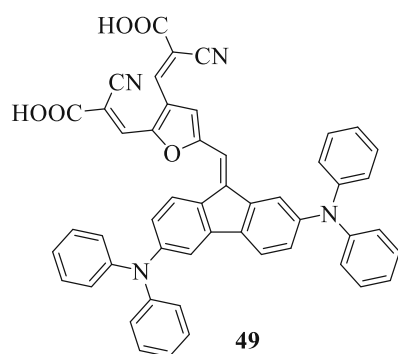
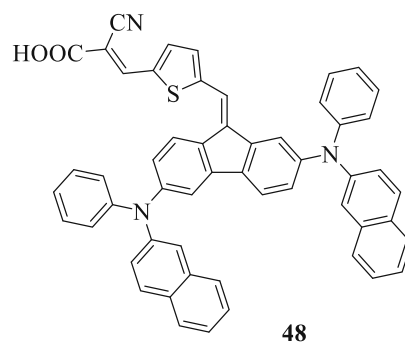
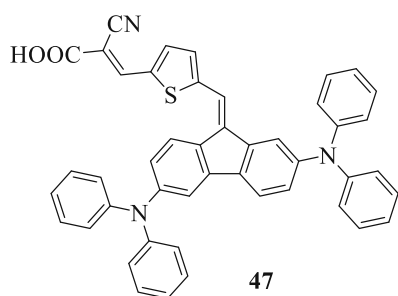
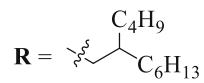
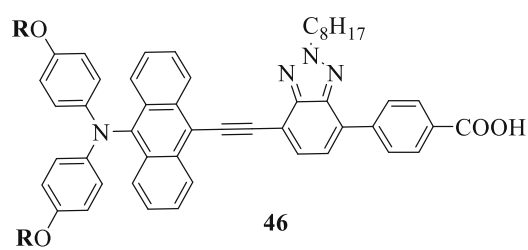
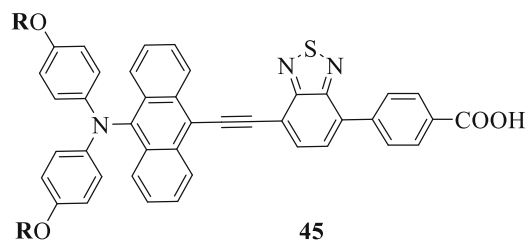
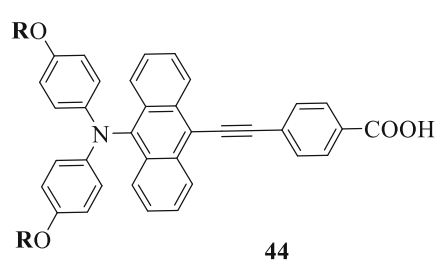
Chemical Structures of the Dyes Used for Room Light DSSCs











CONCLUSION AND PERSPECTIVE

In conclusion, the potential high demand for renewable energy supply for applications in low power consumption will significantly enhance the development of indoor DSSC technology. Recently, a number of attempts have been made to develop indoor DSSCs with a view to achieving highest efficiencies. Professionals from universities, researchers, government and the PV industry work relentlessly to produce new materials that can improve the performance of the indoor DSSC. This review explains the basics of DSSC and discusses recent progress in DSSC photoanodes, sensitizers, electrolytes, and CEs for indoor applications. Usually, indoor lights produce lower light intensity based on the design and lighting mechanisms, with varying emission spectra. Among the numerous indoor lighting sources, LED and fluorescent lamps are the most energy efficient light for our everyday lives, which in most indoor DSSC cases also displayed the highest efficiency because of their narrower spectral widths without the low-photon-energy infrared emission. Actually, most DSSC-based works have been assessed under a standard AM 1.5G condition. In fact, the various light sources are utilized across different types of labs and the illumination state of the indoor atmosphere is different, as is the characteristic of spectrum and intensity. To the best of our knowledge indoor DSSC lighting requirements are not standardized; this includes the light source type, light intensity, etc. No measuring system has yet been developed and validated for evaluating the characteristics of the indoor DSSC.

This review suggests that if sufficient consideration is paid to all four parts of DSSC through the use of highly efficient materials and development techniques, a high-efficiency indoor DSSC could be made and this could be of great commercial interest. For producing optimal dyes for indoor DSSC, it is desirable to raise the amount of alkyl chains on the sensitizers to lift the V_{OC} of the device. The sensitizer's absorption range would also align with the indoor light emission spectra. The optimal dye under indoor lighting does not require either a long conjugation framework or a strong dipole because the emission spectrum of indoor light does not cover the NIR region as opposed to the solar spectrum. This dramatically lowers the synthetic costs of the dyes. Photoanode mesoporous layers should be modified in thickness and the light-scattering capacity to optimize light harvesting and decrease recombination loss. A compact blocking layer is also necessary to prevent electron leakage across a broad spectrum of intensities, allowing the DSSCs to function efficiently in low-light conditions. The long-term stability of the indoor DSSC will help a step towards its commercialization. The liquid electrolyte-based DSSCs show poor stability because of its electrolyte leakage, and organic solvent

evaporation, leading to poor efficiency. The use of polymer based electrolyte could improve the stability of indoor DSSC. Polymers, low-cost nanoparticles, carbon materials or its composites with high catalytic activity, conductivity, and stability can be used as an alternative for Pt based CEs.

FUNDING

Open access funding provided by Manipal Academy of Higher Education, Manipal.

CONFLICT OF INTEREST

We have no conflict of interest to declare

OPEN ACCESS

This article is licensed under a Creative Commons Attribution 4.0 International License, which permits use, sharing, adaptation, distribution and reproduction in any medium or format, as long as you give appropriate credit to the original author(s) and the source, provide a link to the Creative Commons licence, and indicate if changes were made. The images or other third party material in this article are included in the article's Creative Commons licence, unless indicated otherwise in a credit line to the material. If material is not included in the article's Creative Commons licence and your intended use is not permitted by statutory regulation or exceeds the permitted use, you will need to obtain permission directly from the copyright holder. To view a copy of this licence, visit <http://creativecommons.org/licenses/by/4.0/>.

REFERENCES

1. G. Bazan, *Electron. Green J.* 1 (1997).
2. S. Ashina, J. Fujino, T. Masui, T. Ehara, and G. Hibino, *Energy Policy* 41, 584 (2012).
3. U. Ahmed, M. Alizadeh, N.A. Rahim, S. Shahabuddin, M.S. Ahmed, and A.K. Pandey, *Sol. Energy* 174, 1097 (2018).
4. M. Yoosuf, S.C. Pradhan, S. Soman, and K.R. Gopidas, *Sol. Energy* 188, 55 (2019).
5. H. Wu, X. Xie, J. Zhang, S. Li, Z. Shen, and Y. Yuan, *J. Power Sources* 451, 227748 (2020).
6. L. Han, Y. Chen, J. Zhao, Y. Cui, and S. Jiang, *Tetrahedron* 76, 131102 (2020).
7. M.A. Green, *Phys. E Low-Dimensional Syst. Nanostructures* 14, 65 (2002).
8. N.D. Desai, S.S. Mali, R.M. Mane, V.B. Ghanwat, C.K. Hong, and P.N. Bhosale, *J. Mater. Sci. Mater. Electron.* 27, 11739 (2016).
9. S.S. Patil, R.M. Mane, S.S. Mali, C.K. Hong, and P.N. Bhosale, *Sol. Energy* 201, 102 (2020).
10. V.T. Chebrolu, and H. Kim, *J. Mater. Chem. C* 7, 4911 (2019).
11. H.A. Maddah, V. Berry, and S.K. Behura, *Renew. Sustain. Energy Rev.* 121, 109678 (2020).
12. I.M. Abdellah, and A. El-Shafei, *Sol. Energy* 198, 25 (2020).
13. N. Duvva, U. Chilakamarthi, and L. Giribabu, *Sustain. Energy Fuels* 1, 678 (2017).
14. G. Wang, J. Deng, X. Wang, J. Liu, Y. Chen, and B. Liu, *J. Mater. Sci. Mater. Electron.* 30, 20525 (2019).
15. I. Repins, M.A. Contreras, B. Egaas, C. DeHart, J. Scharf, C.L. Perkins, B. To, and R. Noufi, *Prog. Photovoltaics Res. Appl.* 16, 235 (2008).

16. K.L. Chopra, P.D. Paulson, and V. Dutta, *Prog. Photovoltaics Res. Appl.* 12, 69 (2004).
17. M. Saliba, T. Matsui, K. Domanski, J.-Y. Seo, A. Ummadisingu, S.M. Zakeeruddin, J.-P. Correa-Baena, W.R. Tress, A. Abate, A. Hagfeldt, and M. Grätzel, *Science* 354, 206 (2016).
18. J.J. Yoo, S. Wieghold, M.C. Sponseller, M.R. Chua, S.N. Bertram, N.T.P. Hartono, J.S. Tresback, E.C. Hansen, J.P. Correa-Baena, V. Bulović, T. Buonassisi, S.S. Shin, and M.G. Bawendi, *Energy Environ. Sci.* 12, 2192 (2019).
19. H. Ren, S. Yu, L. Chao, Y. Xia, Y. Sun, S. Zuo, F. Li, T. Niu, Y. Yang, H. Ju, B. Li, H. Du, X. Gao, J. Zhang, J. Wang, L. Zhang, Y. Chen, and W. Huang, *Nat. Photonics* 14, 154 (2020).
20. L. Zhou, J. Chang, Z. Liu, X. Sun, Z. Lin, D. Chen, C. Zhang, J. Zhang, and Y. Hao, *Nanoscale* 10, 3053 (2018).
21. J. Feng, X. Zhu, Z. Yang, X. Zhang, J. Niu, Z. Wang, S. Zuo, S. Priya, S. FrankLiu, and D. Yang, *Adv. Mater.* 30, 1 (2018).
22. B.O. Regan, and M. Grätzel, *Nature* 353, 737 (1991).
23. C. Altinkaya, A. Atli, A. Atilgan, K. Salimi, and A. Yildiz, *Int. J. Energy Res.* 44, 3160 (2020).
24. M. Baro, Jaidev, and S. Ramaprabhu, *Appl. Surf. Sci.* 503, 144069 (2020).
25. X. Wang, A. Bolag, W. Yun, Y. Du, C. Eerdun, X. Zhang, T. Bao, J. Ning, H. Alata, and T. Ojayed, *J. Mol. Struct.* 1206, 127694 (2020).
26. M.L. Jiang, J.J. Wen, Z.M. Chen, W.H. Tsai, T.C. Lin, T.J. Chow, and Y.J. Chang, *Chem. Sus. Chem.* 12, 3654 (2019).
27. T.S. Bramhankar, S.S. Pawar, J.S. Shaikh, V.C. Gunge, N.I. Beedri, P.K. Baviskar, H.M. Pathan, P.S. Patil, R.C. Kambale, and R.S. Pawar, *J. Alloys Compd.* 817, 152810 (2020).
28. K. Subalakshmi, and J. Senthilselvan, *Sol. Energy* 171, 914 (2018).
29. S.V. Kuppu, A.R. Jeyaraman, P.K. Guruviah, and S. Thambusamy, *Curr. Appl. Phys.* 18, 619 (2018).
30. C.Y. Tan, F.S. Omar, N.M. Saidi, N.K. Farhana, S. Ramesh, and K. Ramesh, *Sol. Energy* 178, 231 (2019).
31. S.M.J. Nabavi, B. Hosseinzadeh, M. Tajbakhsh, and H. Alinezhad, *J. Mater. Sci. Mater. Electron.* 29, 3270 (2018).
32. A. Aslam, U. Mehmood, M. H. Arshad, A. Ishfaq, J. Zaheer, A. Ul Haq Khan, and M. Sufyan, *Sol. Energy* 207, 874 (2020).
33. I. Mora-Seró, M. Saliba, and Y. Zhou, *Sol. RRL* 4, 1900563 (2020).
34. L. Meng, J. You, and Y. Yang, *Nat. Commun.* 9, 5265 (2018).
35. L. Qiu, L.K. Ono, and Y. Qi, *Energy* 7, 169 (2018).
36. I. Etxebarria, J. Ajuria, and R. Pacios, *J. Photonics Energy* 5, 57214 (2015).
37. M. Grätzel, *Inorg. Chem.* 44, 6841 (2005).
38. C.-P. Lee, C.-T. Li, and K.-C. Ho, *Mater. Today* 20, 267 (2017).
39. U. Mehmood, Z. Malaibari, F.A. Rabani, A.U. Rehman, S.H.A. Ahmad, M.A. Atieh, and M.S. Kamal, *Electrochim. Acta* 203, 162 (2016).
40. S. Iwata, S. Shibakawa, N. Imawaka, and K. Yoshino, *Energy Reports* 4, 8 (2018).
41. L. Fraas and L. Partain, *Solar cells and their applications: Second Edition* (2010).
42. M. Freitag, J. Teuscher, Y. Saygili, X. Zhang, F. Giordano, P. Liska, J. Hua, S.M. Zakeeruddin, J.E. Moser, M. Grätzel, and A. Hagfeldt, *Nat. Photonics* 11, 372 (2017).
43. A.H. Ngu, M. Gutierrez, V. Metsis, S. Nepal, and Q.Z. Sheng, *IEEE Internet Things J.* 4, 1 (2017).
44. A. Raj, and D. Steingart, *J. Electrochem. Soc.* 165, B3130 (2018).
45. S. Venkatesan, I.P. Liu, C.W. Li, C.M. Tseng-Shan, Y.L. Lee, and A.C.S. Sustain, *Chem. Eng. J.* 7, 7403 (2019).
46. S. Biswas, and H. Kim, *Polymers (Basel)*. 12, 1338 (2020).
47. A. Venkateswararao, J.K.W. Ho, S.K. So, S.-W. Liu, and K.-T. Wong, *Mater. Sci. Eng. R Rep.* 139, 100517 (2020).
48. V. Sugathan, E. John, and K. Sudhakar, *Renew. Sustain. Energy Rev.* 52, 54 (2015).
49. L.L. Li, and E.W.G. Diau, *Chem. Soc. Rev.* 42, 291 (2013).
50. J.S. Luo, Z.Q. Wan, and C.Y. Jia, *Chinese Chem. Lett.* 27, 1304 (2016).
51. A. Mahmood, *Sol. Energy* 123, 127 (2016).
52. J. Gong, K. Sumathy, Q. Qiao, and Z. Zhou, *Renew. Sustain. Energy Rev.* 68, 234 (2017).
53. M.R. Narayan, *Renew. Sustain. Energy Rev.* 16, 208 (2011).
54. M.K. Nazeeruddin, E. Baranoff, and M. Grätzel, *Sol. Energy* 85, 1172 (2011).
55. M.E. Yeoh, and K.Y. Chan, *Int. J. Energy Res.* 41, 2446 (2017).
56. B. Roose, S. Pathak, and U. Steiner, *Chem. Soc. Rev.* 44, 8326 (2015).
57. S. Yun, Y. Qin, A.R. Uhl, N. Vlachopoulos, M. Yin, D. Li, X. Han, and A. Hagfeldt, *Energy Environ. Sci.* 11, 476 (2018).
58. J. Gong, J. Liang, and K. Sumathy, *Renew. Sustain. Energy Rev.*
59. A. Hagfeldt, and M. Graetzel, *Chem. Rev.* 95, 49 (1995).
60. S. Rühle, and D. Cahen, *J. Phys. Chem. B* 108, 17946 (2004).
61. Y.-C. Chen, Y.-C. Chang, and C.-M. Chen, *J. Electrochem. Soc.* 165, F409 (2018).
62. K.W. Chen, L.S. Chen, and C.M. Chen, *J. Mater. Sci. Mater. Electron.* 30, 15105 (2019).
63. J.C. Chou, C.H. Kuo, P.Y. Kuo, C.H. Lai, Y.H. Nien, Y.H. Liao, C.C. Ko, C.M. Yang, and C.Y. Wu, *IEEE J. Photovoltaics* 9, 926 (2019).
64. C. Hora, F. Santos, M.G.F. Sales, D. Ivanou, A. Mendes, and A.C.S. Sustain, *Chem. Eng. J.* 7, 13464 (2019).
65. I.P. Liu, W.H. Lin, C.M. Tseng-Shan, Y.L. Lee, and A.C.S. Appl, *Mater. Interfaces* 10, 38900 (2018).
66. Y.-H. Nien, H.-H. Chen, H.-H. Hsu, M. Rangasamy, G.-M. Hu, Z.-R. Yong, P.-Y. Kuo, J.-C. Chou, C.-H. Lai, C.-C. Ko, and J.-X. Chang, *Energies* 13, 2248 (2020).
67. S. Sasidharan, S. C. Pradhan, A. Jagadeesh, B. N. Nair, A. A. P. Mohamed, N. U. K. N, S. Soman, and U. N. S. Harceeh, *ACS Appl. Energy Mater.* 3, 12584 (2020).
68. C.Y. Chen, Z.H. Jian, S.H. Huang, K.M. Lee, M.H. Kao, C.H. Shen, J.M. Shieh, C.L. Wang, C.W. Chang, B.Z. Lin, C.Y. Lin, T.K. Chang, Y. Chi, C.Y. Chi, W.T. Wang, Y. Tai, M. De Lu, Y.L. Tung, P.T. Chou, W.T. Wu, T.J. Chow, P. Chen, X.H. Luo, Y.L. Lee, C.C. Wu, C.M. Chen, C.Y. Yeh, M.S. Fan, J. De Peng, K.C. Ho, Y.N. Liu, H.Y. Lee, C.Y. Chen, H.W. Lin, C. Te Yen, Y.C. Huang, C.S. Tsao, Y.C. Ting, T.C. Wei, and C.G. Wu, *J. Phys. Chem. Lett.* 8, 1824 (2017).
69. C.H. Huang, Y.W. Chen, C.M. Chen, and A.C.S. Appl, *Mater. Interfaces* 10, 2658 (2018).
70. T.D. Nguyen, C.H. Lin, C.L. Mai, and C.G. Wu, *ACS Omega* 4, 11414 (2019).
71. C.V. Jagtap, V.S. Kadam, S.R. Jadkar, and H.M. Pathan, *ES Energy Environ.* 3, 60 (2019).
72. J.L. Lan, T.C. Wei, S.P. Feng, C.C. Wan, and G. Cao, *J. Phys. Chem. C* 116, 25727 (2012).
73. S. Venkatesan, W.H. Lin, H. Teng, Y.L. Lee, and A.C.S. Appl, *Mater. Interfaces* 11, 42780 (2019).
74. S. Venkatesan, I.P. Liu, J.C. Lin, M.H. Tsai, H. Teng, and Y.L. Lee, *J. Mater. Chem. A* 6, 10085 (2018).
75. I.P. Liu, W.N. Hung, H. Teng, S. Venkatesan, J.C. Lin, and Y.L. Lee, *J. Mater. Chem. A* 5, 9190 (2017).
76. S. Venkatesan, S.C. Su, W.N. Hung, I.P. Liu, H. Teng, and Y.L. Lee, *J. Power Sources* 298, 385 (2015).
77. S.J. Seo, H.J. Cha, Y.S. Kang, and M.S. Kang, *Electrochim. Acta* 145, 217 (2014).
78. S. Venkatesan, I.P. Liu, W.N. Hung, H. Teng, and Y.L. Lee, *Chem. Eng. J.* 367, 17 (2019).
79. S. Venkatesan, I. P. Liu, C. M. Tseng Shan, H. Teng, and Y. L. Lee, *Chem. Eng. J.* 394, 124954 (2020).
80. I.-P. Liu, Y.-Y. Chen, Y.-S. Cho, L.-W. Wang, C.-Y. Chien, and Y.-L. Lee, *J. Power Sources* 482, 228962 (2021).
81. M. Wu, and T. Ma, *Chem. Sus. Chem.* 5, 1343 (2012).

82. M. Wu, X. Lin, Y. Wang, L. Wang, W. Guo, D. Qi, X. Peng, A. Hagfeldt, M. Grätzel, and T. Ma, *J. Am. Chem. Soc.* 134, 3419 (2012).
83. M.H. Yeh, L.Y. Lin, C.P. Lee, H.Y. Wei, C.Y. Chen, C.G. Wu, R. Vittal, and K.C. Ho, *J. Mater. Chem.* 21, 19021 (2011).
84. C.P. Lee, C.A. Lin, T.C. Wei, M.L. Tsai, Y. Meng, C.T. Li, K.C. Ho, C.I. Wu, S.P. Lau, and J.H. He, *Nano Energy* 18, 109 (2015).
85. Y.J. Huang, H.T. Chen, S.B. Ann, C.T. Li, J.T. Lin, C.P. Lee, and K.C. Ho, *J. Mater. Chem. A* 7, 26089 (2019).
86. Y.J. Huang, Y.J. Lin, H.J. Chien, Y.F. Lin, and K.C. Ho, *Nanoscale* 11, 12507 (2019).
87. A. Mishra, M.K.R. Fischer, and P. Büuerle, *Angew. Chemie Int. Ed.* 48, 2474 (2009).
88. J.M. Ji, H. Zhou, and H.K. Kim, *J. Mater. Chem. A* 6, 14518 (2018).
89. C.H. Chen, P.T. Chou, T.C. Yin, K.F. Chen, M.L. Jiang, Y.J. Chang, C.K. Tai, and B.C. Wang, *Org. Electron.* 59, 69 (2018).
90. M. B. Desta, N. S. Vinh, C. Pavan Kumar, S. Chaurasia, W. T. Wu, J. T. Lin, T. C. Wei, and E. Wei-Guang Diao, *J. Mater. Chem. A* 6, 13778 (2018).
91. M.C. Tsai, C.L. Wang, C.W. Chang, C.W. Hsu, Y.H. Hsiao, C.L. Liu, C.C. Wang, S.Y. Lin, and C.Y. Lin, *J. Mater. Chem. A* 6, 1995 (2018).
92. M. C. Tsai, Y. C. Chiu, M. De Lu, Y. L. Tung, H. C. Tsai, J. R. Chang Chien, and C. Y. Lin, *ACS Appl. Energy Mater.* 3, 2744 (2020).
93. H.H. Chou, Y.C. Liu, G. Fang, Q.K. Cao, T.C. Wei, C.Y. Yeh, and A.C.S. Appl, *Mater. Interfaces* 9, 37786 (2017).
94. R. Y. Huang, W. H. Tsai, J. J. Wen, Y. J. Chang, and T. J. Chow, *J. Power Sources* 458, 228063 (2020).
95. C.T. Li, Y.L. Kuo, C.P. Kumar, P.T. Huang, and J.T. Lin, *J. Mater. Chem. A* 7, 23225 (2019).
96. K.S.K. Reddy, Y.C. Chen, C.C. Wu, C.W. Hsu, Y.C. Chang, C.M. Chen, C.Y. Yeh, and A.C.S. Appl, *Mater. Interfaces* 10, 2391 (2018).
97. E. Tanaka, H. Michaels, M. Freitag, and N. Robertson, *J. Mater. Chem. A* 8, 1279 (2020).
98. Y. S. Tingare, N. S. n. Vinh, H. H. Chou, Y. C. Liu, Y. S. Long, T. C. Wu, T. C. Wei, and C. Y. Yeh, *Adv. Energy Mater.* 7, 30 (2017).
99. Y.C. Chen, G.W. Huang, Y.J. Chang, and J.J. Wen, *J. Mater. Sci. Mater. Electron.* 30, 12981 (2019).
100. M. Chandra Sil, L.-S. Chen, C.-W. Lai, Y.-H. Lee, C.-C. Chang, and C.-M. Chen, *J. Power Sources* 479, 229095 (2020).

Publisher's Note Springer Nature remains neutral with regard to jurisdictional claims in published maps and institutional affiliations.